

# Pleiotropic actions of miR-21 highlight the critical role of deregulated stromal microRNAs during colorectal cancer progression

This article has been corrected since Online Publication and a corrigendum has also been published

MD Bullock<sup>\*1</sup>, KM Pickard<sup>1</sup>, BS Nielsen<sup>2</sup>, AE Sayan<sup>1</sup>, V Jenei<sup>1</sup>, M Mellone<sup>1</sup>, R Mitter<sup>3</sup>, JN Primrose<sup>1</sup>, GJ Thomas<sup>1</sup>, GK Packham<sup>1</sup> and AH Mirnezami<sup>1</sup>

The oncogene microRNA-21 (miRNA; miR-21) is overexpressed in most solid organ tumours; however, a recent examination of stage II colorectal cancer (CRC) specimens suggests this may be a stromal phenomenon and not only a feature of cancer cells. *In vitro* and *in vivo* studies show that miR-21 has potent pro-metastatic effects in various malignant carcinoma cell lines. The tumour microenvironment has also been identified as a key actor during the metastatic cascade; however to date the significance of deregulated miR-21 expression within the cancer-associated stroma has not been examined. In the present study, a quantitative RT-PCR-based analysis of laser microdissected tissue confirmed that miR-21 expression is associated with a four-fold mean increase in CRC stroma compared with normal tissue. *In situ* hybridisation using locked nucleic acid probes localised miR-21 expression predominantly to fibroblasts within tumour-associated stroma. To study the molecular and biological impact of deregulated stromal miR-21 in CRC, stable ectopic expression was induced in immortalised fibroblasts. This resulted in upregulated  $\alpha$ -smooth muscle actin expression implying miR-21 overexpression is driving the fibroblast-to-myofibroblast transdifferentiation. Conditioned medium from miR-21-overexpressing fibroblasts protected CRC cells from oxaliplatin-induced apoptosis and increased their proliferative capacity. 3D organotypic co-cultures containing fibroblasts and CRC cells revealed that ectopic stromal miR-21 expression was associated with increased epithelial invasiveness. Reversion-inducing cysteine-rich protein with kazal motifs, an inhibitor of matrix-remodelling enzyme MMP2, was significantly downregulated by ectopic miR-21 in established and primary colorectal fibroblasts with a reciprocal rise in MMP2 activity. Inhibition of MMP2 abrogated the invasion-promoting effects of ectopic miR-21. This data, which characterises a novel pro-metastatic mechanism mediated by miR-21 in the CRC stroma, highlights the importance of miRNA deregulation within the tumour microenvironment and identifies a potential application for stromal miRNAs as biomarkers in cancer.

*Cell Death and Disease* (2013) 4, e684; doi:10.1038/cddis.2013.213; published online 20 June 2013

**Subject Category:** Cancer

Colorectal cancer (CRC) is a key public health issue, and accounts for the second highest cause of cancer-related death in Western societies.<sup>1</sup> Metastases are the principle cause of death, and occur in 30% of patients at presentation and subsequently in >50% of patients after surgery with curative intent.<sup>2</sup> The metastatic cascade is a complex, multistep process<sup>3</sup> and despite the introduction of chemotherapy and newer targeted therapies, the majority of patients with metastases remain incurable.<sup>4,5</sup> An important feature of metastatic progression is the role had by the tumour microenvironment and the promotion of tumour growth, invasion and angiogenesis by the cancer-associated stroma.<sup>6,7</sup> The key cellular components of

cancer-associated stroma are myofibroblasts,  $\alpha$ -smooth muscle actin (SMA)-expressing cells that transdifferentiate from fibroblast progenitors in response to paracrine signals from the malignant epithelium.<sup>6</sup> These cells also modulate the chemistry of the tumour microenvironment by producing matrix metalloproteinase enzymes (MMPs), MMP inhibitors, extracellular matrix (ECM) components, growth factors and cytokines.<sup>8</sup> The dynamic and reciprocal interaction between stromal and malignant epithelial cells has a profound impact on tumour progression *in vivo*,<sup>9</sup> and as stromal cells are less likely to acquire *de novo* mutations, evade anti-cancer immunity or develop drug resistance, the development of targeted therapies based on improved

<sup>1</sup>Cancer Sciences Division, University of Southampton, Somers Cancer Sciences Building, Southampton General Hospital, Tremona Road, Southampton, UK; <sup>2</sup>Bioneer A/S, Molecular Histology, Horsholm, Denmark and <sup>3</sup>Bioinformatics Unit, London Research Institute, Cancer Research UK, London, UK

\*Corresponding author: MD Bullock, Cancer Sciences Division, University of Southampton, Somers Cancer Sciences Building, Southampton General Hospital, Tremona Road, Southampton SO16 6YD, UK. Tel: +44 (0)772 0896 567; Fax: +44 (0)238 0794 020; E-mail: m.bullock@soton.ac.uk

**Keywords:** colorectal neoplasia; neoplasm metastasis; stroma; MicroRNA; MiR-21

**Abbreviations:** miRNA (miR), microRNA; CRC, colorectal cancer; MMP, matrix metalloproteinase; ECM, extracellular matrix; PTEN, phosphate and tensin homologue; PDCD4, programmed cell death 4; RECK, reversion-inducing cysteine-rich protein with kazal motifs; TGF- $\beta$ , transforming growth factor beta; ISH, *in situ* hybridisation; LNA, locked nucleic acid; LMD, laser microdissection; qPCR, quantitative PCR; SMA, smooth muscle actin; CM, conditioned medium; GFP, green fluorescent protein; PCF, primary colon fibroblast; FFPE, formalin-fixed paraffin-embedded; DMEM, Dulbecco's modified Eagle medium; FBS, foetal bovine serum; VIM, vimentin; CDH1, E-Cadherin; S100A4 (FSP1), S100 calcium-binding protein A4 (fibroblast-specific protein 1)

Received 10.4.13; revised 13.5.13; accepted 17.5.13; Edited by M Agostini

molecular characterisation of CRC stroma is an attractive prospect.<sup>10,11</sup>

MicroRNAs (miRNAs) are a class of small highly conserved non-coding RNAs that provide widespread expressional control through repression of mRNA translation. They are strongly implicated in the pathogenesis of numerous malignancies,<sup>12</sup> and hold promise as therapeutic targets as they regulate fundamental intracellular processes and are deregulated, often in a tissue- and tumour-specific manner, in all cancer types examined to date.<sup>13</sup>

In CRC, miRNAs derail a number of cellular signal transduction and cell survival pathways including the Wnt/ $\beta$ -catenin pathway, epidermal growth factor receptor pathway and p53 function connecting miRNA biology to known mutational events in the classical adenoma–carcinoma sequence of malignant transformation and potentially to each of the hallmarks of cancer.<sup>14</sup>

High throughput profiling studies have also uncovered miRNA-mediated pathways in the regulation of metastasis. One miRNA with particular prominence is miRNA-21 (miR-21), which in diverse cancer cell lines regulates apoptosis and metastasis by suppressing genes such as phosphate and tensin homologue (*PTEN*),<sup>15</sup> programmed cell death 4 (*PDCD4*)<sup>16</sup> and MMP inhibitors, reversion-inducing cysteine-rich protein with Kazal motifs, (*RECK*) and tissue inhibitor of metalloproteinase 3.<sup>17</sup>

Interestingly, Nielsen *et al.*<sup>18</sup> recently demonstrated that miR-21 overexpression in stage II CRC occurs in the stroma rather than in the epithelium. In a separate study, miR-21 suppression with antisense inhibitors was shown to prevent the fibroblast-to-myofibroblast transdifferentiation in response to transforming growth factor beta (TGF- $\beta$ ).<sup>19</sup> Together, these data suggest that the pro-metastatic influence of miR-21 may be mediated through the tumour microenvironment; however, biological and functional evidence to support this model has not been deeply investigated.

The aims of the current study are to provide multimodal validation of miR-21 expression patterns in CRC and to gain improved understanding of the pathological relevance of deregulated stromal miR-21 by dissecting out molecular interactions within the tumour microenvironment.

## Results

**MiR-21 expression localises to fibroblast-like cells in the CRC stroma.** Mir-21 has been shown to be upregulated in different cancers including CRC.<sup>20–24</sup> As most of these studies utilised pieces of tumour tissue containing tumour and non-tumour cells for the detection of miR-21 expression, the relative contribution of stromal/cancers cells to the observed miR-21 upregulation is not clearly established. To identify the source of overexpressed miR-21 in CRC, we used an *in situ* hybridisation (ISH) technique. Highly sensitive locked nucleic acid (LNA) probes showed specific and predominant staining in fibroblast-like cells in the stroma of all CRC specimens examined. Crucially, tumour epithelium and benign tissue showed only weak and sporadic expression of miR-21 in mononuclear cells (Figure 1a). To quantify the overexpression of miR-21, we performed laser microdissection (LMD; Figure 1b) followed by quantitative PCR

(qPCR) using TaqMan probes (Applied Biosystems, Foster City, CA, USA). We found that mean miR-21 expression was fourfold higher in the LMD stroma of CRC specimens compared with paired normal tissue ( $P=0.005$ , Figure 1c). To prove the efficiency of LMD, we also conducted qPCR assays to quantify expression of epithelial and mesenchymal markers in microdissected tissue. Microdissected stroma expressed high levels of mesenchymal cell-specific vimentin (VIM) mRNA and fibroblast-specific protein 1 (FSP1; S100 calcium-binding protein A4, S100A4;  $P<0.05$ ) and low levels of epithelium-specific E-Cadherin (CDH1;  $P=0.05$ ; Figure 1d).

## The impact of stable ectopic miR-21 overexpression in immortalised stromal fibroblasts.

To assess the biological significance of upregulated stromal miR-21, its ectopic expression was stably induced in an established human fibroblast cell line (MRC5). MiR-21-overexpressing MRC5 cells (MRC5<sup>21</sup>) underwent striking morphological change, adopting enlarged and elongated forms, which was accompanied by minor increases in  $\alpha$ -SMA expression compared with identical passage scrambled control-transfected (MRC5<sup>SCC</sup>) cells (Figure 2a). Fibroblasts showing similar morphological features are considered as myofibroblasts and characterised by increased  $\alpha$ -SMA containing intracellular filaments. Secreted molecules from cancer cells such as TGF- $\beta$  are responsible for fibroblast-to-myofibroblast transdifferentiation.<sup>8</sup> Myofibroblasts are often observed in the tumour microenvironment and their presence has been proposed as an independent marker of poor prognosis.<sup>25</sup>

To assess whether miR-21 overexpression primes myofibroblast transdifferentiation or provokes an intermediate differentiation state, MRC5<sup>21</sup> and MRC5<sup>SCC</sup> cells were treated with conditioned media (CM) extracted from SW480 CRC cells (CM<sup>SW480</sup>) or TGF- $\beta$  at 2 ng/ml or 10 ng/ml final concentration, respectively. After 3 days,  $\alpha$ -SMA expression was assessed by immunofluorescence revealing that stress fibre formation had occurred in a significantly greater proportion of MRC5<sup>21</sup> cells than that of MRC5<sup>SCC</sup> cells in response to CM<sup>SW480</sup> and low dose TGF- $\beta$ . As anticipated, treatment with higher TGF- $\beta$  doses induced large numbers of both MRC5<sup>SCC</sup> and MRC5<sup>21</sup> cells to undergo myofibroblast transdifferentiation. Stress fibre deposition was not found in significant numbers of MRC5<sup>21</sup> or MRC5<sup>SCC</sup> cells in the untreated group (Figure 2b).

These results suggest that although miR-21 expression alone is insufficient to drive myofibroblast transdifferentiation, it may condition/facilitate fibroblasts to acquire the myofibroblast state.

## Medium supernatant from miR-21-overexpressing fibroblasts increases the proliferative capacity of CRC cells and protects them from oxaliplatin-induced apoptosis.

The reciprocal interaction between cancer cells and tumour stroma is a contributing factor in carcinoma progression. To assess the effect of stromal miR-21 manipulation on the cell fate of CRC cells, we investigated their proliferative properties and resistance to apoptosis. After a 24- or 48-h incubation with CM from MRC5<sup>21</sup> cells (CM<sup>21</sup>), the mean cell density of SW480 cells increased by 40% ( $P<0.03$ ) and 93% ( $P=0.01$ ) compared with controls (CM from MRC5<sup>SCC</sup>; CM<sup>SCC</sup>),

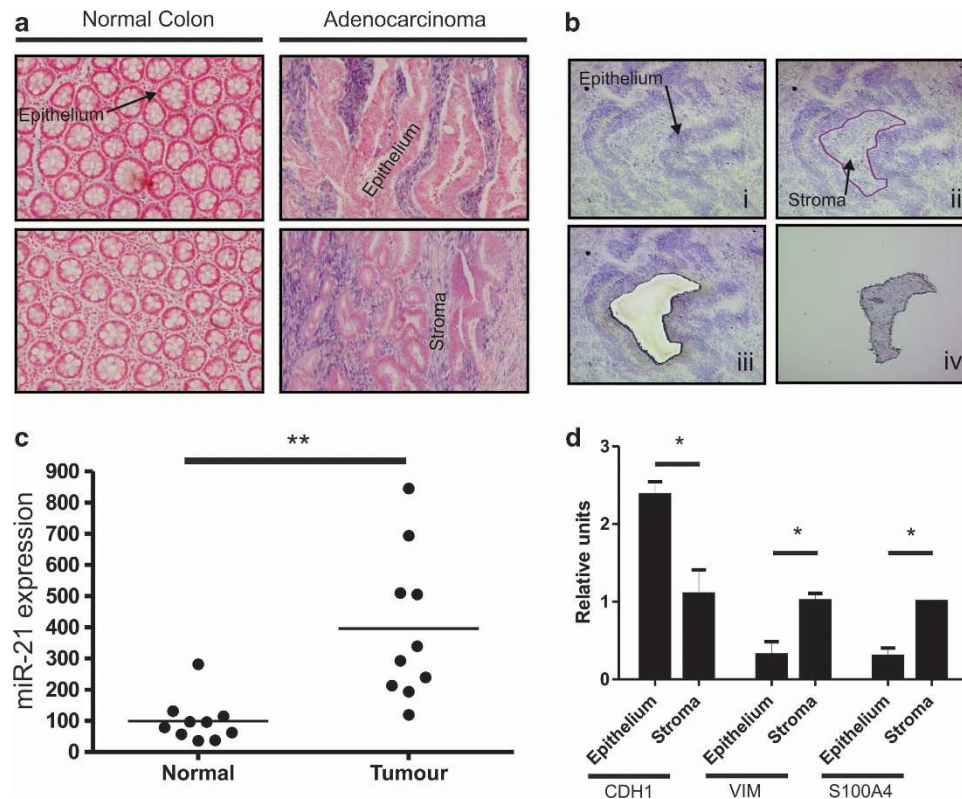


**Figure 1** (a) ISH of representative CRC and normal colonic tissue sections using LNA probes against miR-21. MiR-21 positivity is characterised by an intense blue chromogenic reaction. (b) LMD was performed on fresh frozen human CRC specimens and paired normal tissue to isolate stroma from epithelial tissue. Cresyl violet staining was used to highlight epithelium (i); the area of interest was then defined (ii) before laser dissection occurred (iii) and the cut piece was transported to a collection device (iv). (c) High sensitivity TaqMan qPCR using total RNA extracted from LMD tissue of patients with CRC ( $n = 10$ ) reveals that stromal miR-21 expression successfully separates tumour from paired normal tissue. Absolute miR-21 expression values are displayed around the mean represented by a horizontal bar. (d) To prove the efficiency of LMD, expression of mesenchymal cell-specific mRNA vimentin (VIM), FSP1 mRNA (S100A4), and epithelium-specific mRNA E-Cadherin (CDH1) were quantified in LMD stromal and epithelial tissue (\* $P < 0.05$ ; \*\* $P < 0.005$ )

respectively. Under the same conditions, another CRC cell line (DLD1) showed an 18% ( $t = 24$  h,  $P = 0.09$ ) and 66% ( $t = 48$  h,  $P = 0.01$ ) mean cell density increase compared with controls (Figure 3a).

We also evaluated the comparative effect of CM<sup>21</sup> or CM<sup>SCC</sup> treatment on oxaliplatin-mediated apoptosis. We found that oxaliplatin, a first-line cytotoxic agent for the treatment of patients with stage III and IV CRC, was less effective at inducing apoptosis and cell death in CM<sup>21</sup>-treated CRC cells compared with CM<sup>SCC</sup>-treated controls (Figures 3b and c).

**Medium supernatant from miR-21-overexpressing fibroblasts enhances CRC cell invasion.** Increased motility and invasion are critical physiological processes in the course of metastasis. To assess whether stromal miR-21 alters the invasive properties of CRC cells, we used CM from miR-21 and miR-SCC stably transfected cells (CM<sup>21</sup>/CM<sup>SCC</sup>) as chemoattractant and performed transwell invasion assays. CM<sup>21</sup> was associated with 1.7- ( $P < 0.02$ ) and 1.8-fold ( $P = 0.03$ ) increases in invasiveness of SW480 and DLD1 CRC epithelial cells, respectively, compared with CM<sup>SCC</sup> controls (Figure 4a). In order to examine invasiveness further, we used organotypic culture conditions that

closely resemble the *in vivo* tumour microenvironment. To achieve this, we embedded MRC5<sup>21</sup> or MRC5<sup>SCC</sup> cells into gels containing ECM components (matrigel and collagen) and seeded CRC cells as a layer on the top. Our results showed a 2.5-fold ( $P < 0.005$ ) increase in the invasion of SW480 cells into the stroma containing MRC5<sup>21</sup> cells compared with control (Figure 4b). Green fluorescent protein (GFP)-positive cells within the stroma confirmed the presence of fibroblasts stably transfected with IRES-driven miRNA/GFP co-expression plasmid (Figure 4c). These results suggest that stromal expression of miR-21 can induce enhanced motility and invasion of CRC cells.

**MiR-21 targets RECK in the CRC stroma.** To streamline the search for mechanistic explanations for the novel observation that miR-21 overexpression in fibroblasts enhances CRC invasiveness, we turned our focus to a regulator of ECM remodelling known to be targeted by miR-21.<sup>17</sup> RECK is a negative regulator of MMP activity. RECK mRNA has been shown to be targeted directly by miR-21 in mutated/unmutated 3'-untranslated region luciferase reporter assays in several cell lines and in numerous tumour contexts.<sup>17,26</sup> We found that stable miR-21-expressing fibroblasts express reduced RECK mRNA and protein

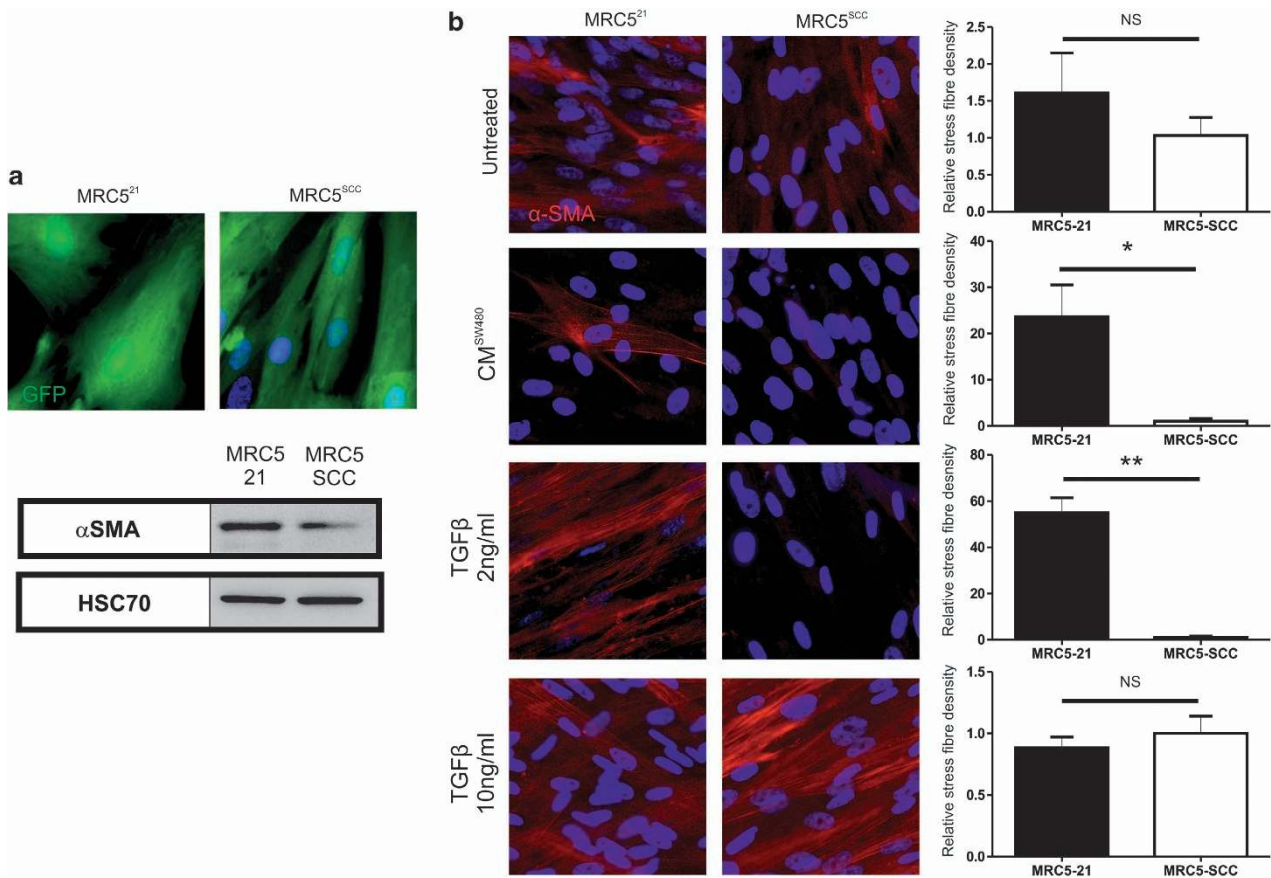


**Figure 2** Fluorescence from MRC5 fibroblasts stably transfected with miR-21/GFP or control miR-SCC/GFP co-expression plasmids highlight the morphological changes associated with ectopic miR-21 expression in fibroblasts ( $\times 40$  magnification). Western blot analysis reveals that MRC5 fibroblasts in which miR-21 has been stably induced express upregulated  $\alpha$ -SMA compared with controls. (b) Immunofluorescence staining for  $\alpha$ -SMA in MRC5 fibroblasts stably expressing either miR-21 or miR-SCC at  $\times 40$  magnification: MiR-21 but not miR-SCC is associated with  $\alpha$ -SMA stress fibres formation, following treatment with low doses of TGF- $\beta$  (2 ng/ml) or culture medium extracted from SW480 CRC cells (CM<sup>SW480</sup>). High doses of TGF- $\beta$  (10 ng/ml) also induce stress fibre deposition in miR-SCC-transfected cells, which serves as a positive control (\* $P < 0.05$ ; \*\* $P < 0.005$ )

(Figures 5a and b). These results provide mechanistic explanation why stromal expression of miR-21 is a contributing factor to invasiveness of CRC tumours. In order to validate the functional consequences of miR-21 expression in relation to MMP activation, we stained sections of organotypic cultures with RECK. We observed fibroblast-specific expression of this protein in MRC5<sup>SCC</sup> but not MRC5<sup>21</sup> specimens consistent with our previous findings that MRC5<sup>21</sup>-containing stroma significantly enhanced invasion of SW480 CRC cells (Figure 5c).

Finally, to observe the relationship between miR-21 and its target RECK in a more physiological setting, primary colon fibroblasts (PCFs) were obtained and transiently transfected with miR-21/GFP or miR-SCC/GFP co-expression plasmid. After 48 h, transfection cells were fixed for the purpose of immunofluorescence labelling. Cells transfected with scrambled control plasmid demonstrated baseline RECK expression. In contrast, miR-21-transfected cells displayed decreased RECK expression in proportion with transfection efficiency as cells exhibiting the most intense GFP signal were also associated with the most diminished RECK fluorescence signal (Figure 5d).

**MiR-21-dependent RECK downregulation is associated with a reciprocal rise in MMP2 activity – CRC invasion is MMP2 dependent.** The key action of RECK is to inhibit the otherwise unchecked activity of MMPs involved in the breakdown of ECM. To assess whether RECK downregulation in response to ectopic miR-21 expression leads to increased MMP activity, CM<sup>21</sup> and CM<sup>SCC</sup> were analysed by gelatin zymography. In this assay, a dominant band corresponding to MMP2 was consistently detected and miR-21 upregulation led to a significantly increased gelatinase activity compared with controls (Figures 6a and b).

Importantly, the increased invasive effect associated with CM<sup>21</sup> compared with CM<sup>SCC</sup> in transwell assays was partially abrogated in the presence of 25  $\mu$ M MMP2 inhibitor (Figure 6c), suggesting stromal miR-21-dependent SW480 CRC cell invasion is mediated in part by increased MMP2 activity.

## Discussion

Targeted therapeutic strategies based on an improved understanding of the molecular biology of malignancy have been applied to CRC with little success;<sup>4,5</sup> however, recent

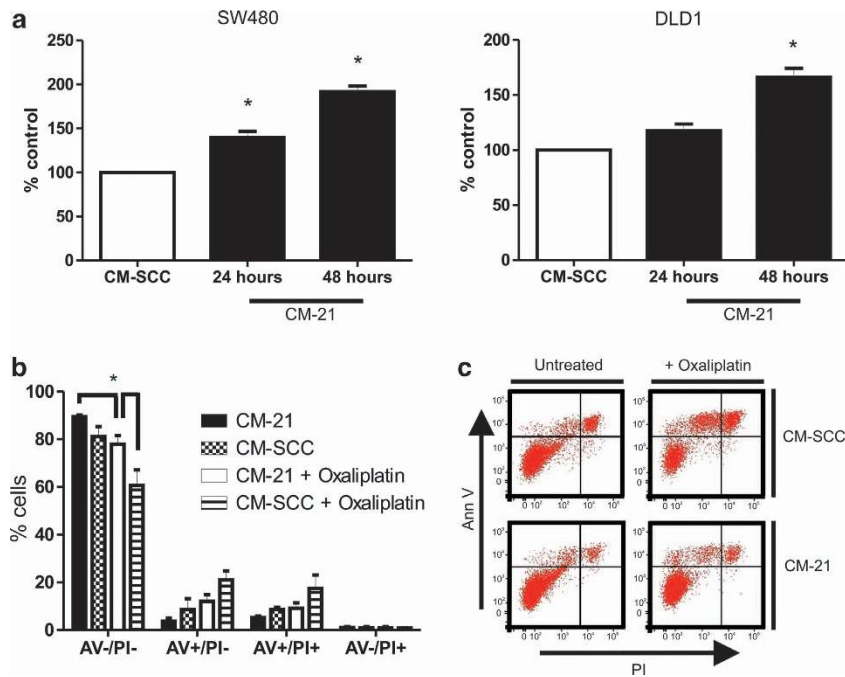


**Figure 3** (a) Cell proliferation and viability assay of SW480 and DLD1 CRC cells following treatment with CM<sup>21</sup> or CM<sup>SCC</sup>. Results represent mean cell density  $\pm$  S.E.M. after 24 or 48 h incubation, from experiments repeated in triplicate. (b) Analysis of apoptosis in SW480 CRC cells pre-treated with CM<sup>21</sup> or CM<sup>SCC</sup> in the presence or absence of oxaliplatin at 30  $\mu$ g/ml. Columns represent percentage of live (AV - /PI -), early apoptotic (AV + /PI -) and late apoptotic (AV + /PI +) cells in each treatment group. Data presented represents results from three independent experiments expressed as means  $\pm$  S.E.M. (c) Representative FACS plot indicating the quadrants used to calculate the proportion of live and apoptotic cells in b. (\* $P \leq 0.05$ )

insights linking deregulated miRNA expression to malignant change<sup>16,27</sup> and to the acquisition of metastatic capabilities<sup>17,28–31</sup> have brought renewed optimism. Although cancer-associated stroma is an attractive target for novel drug development, researchers have focused mainly on deregulated miRNAs in cancer epithelial cells, and as a consequence the identity and the role of stromal miRNAs remains poorly understood.

Nevertheless, recent studies have provided valuable insights: Bronisz *et al.*<sup>32</sup> powerfully demonstrated that down-regulation of miR-320 in mammary stromal fibroblasts reprograms the tumour microenvironment by activating a pro-oncogenic secretome; and Yao *et al.*<sup>19</sup> demonstrated that myofibroblast transdifferentiation from progenitor fibroblasts in response to TGF- $\beta$  could be prevented using specific antisense inhibitors of miR-21. The implications of these data, which suggest a regulatory role for miRNAs in fibroblast differentiation and phenotype, are potentially profound as cancer-associated fibroblasts, including myofibroblasts, are powerful regulators of invasive cancer growth, angiogenesis and disease progression (reviewed by De Wever *et al.*<sup>8</sup>).

Studies of various solid organ tumours have linked elevated miR-21 expression to advancing tumour stage, venous invasion, lymph node and distant metastases, poor disease-free survival and poor overall survival.<sup>33,34</sup> In CRC cell lines, miR-21 correlates inversely with target protein PDCD4 expression, and anti-miR-21 reduces invasiveness and capacity to form metastases in chicken-embryo-metastasis assays.<sup>16</sup> MiR-21 upregulation enhances proliferation in pancreatic, glioblastoma and CRC cell lines,<sup>20–22</sup> and as a

known anti-apoptotic factor<sup>23</sup> it promotes resistance to radiotherapy and chemotherapy in several tumour contexts.<sup>24</sup>

Crucially however, the chemoresistance and pro-metastatic functions attributed to miR-21 are all mediated by the malignant epithelium.

In the present study, we used high sensitivity TaqMan qPCR assays to demonstrate that upregulated miR-21 expression occurs not in CRC cells but in the cancer-associated stroma. Furthermore, ISH pinpointed miR-21 overexpression exclusively to fibroblast-like cells. Prompted by these results, analysis of upregulated miR-21 expression in the stroma became an important priority. The most striking effect of stable miR-21 expression in MRC5 fibroblasts was the adoption of an elongated and enlarged morphology, accompanied by a minor increase in  $\alpha$ -SMA expression. Although suggestive of myofibroblast differentiation status, in the absence of significant stress fibre deposition, it was essential to conclude that miR-21 overexpression alone is insufficient to drive fibroblast-to-myofibroblast transdifferentiation.

Nevertheless, fibroblasts in which miR-21 had been ectopically expressed did share a number of tumour-promoting characteristics with myofibroblasts. Treatment with CM<sup>21</sup> was associated with increased proliferation and reduced oxaliplatin-induced apoptosis in CRC cell lines. CM<sup>21</sup> was also associated with increased CRC cell invasiveness in *in vitro* transwell invasion assays and organotypic models.

To characterise the mechanism underlying this novel pro-invasive effect, we turned our attention to regulators of ECM remodelling known to be targeted by miR-21. RECK has been shown to be targeted by miR-21 in glioma models, and as a

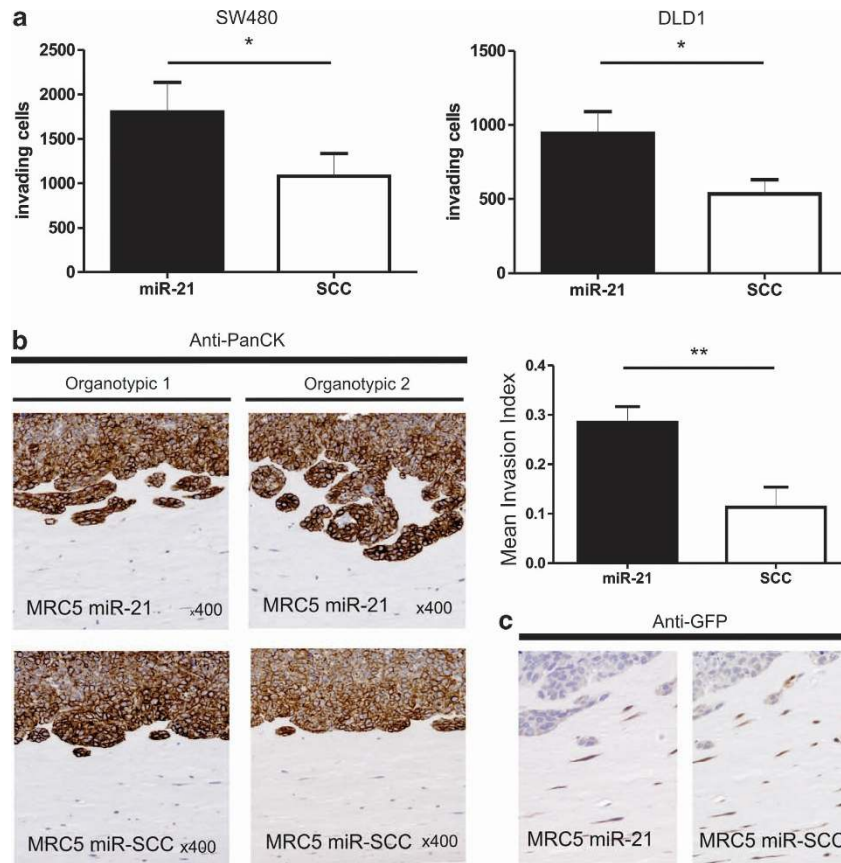


**Figure 4** (a) CM<sup>21</sup> when used as chemoattractant in *in vitro* transwell invasion assays is associated with increased invasiveness in CRC cell lines (SW480 and DLD1) compared with control (CM<sup>SCC</sup>). Data presented represents results from three independent experiments (mean  $\pm$  S.E.M.; \* $P < 0.05$ ). (b) Representative sections of organotypic co-culture models containing MRC5<sup>21</sup> and MRC5<sup>SCC</sup> cells within the stroma. Immunohistochemical staining with anti-pan-Cytokeratin antibody highlights malignant epithelial SW480 CRC cells. The invasion index is increased 2.5-fold in the presence of MRC5<sup>21</sup> cells compared with control-transfected MRC5<sup>SCC</sup> cells (mean  $\pm$  S.E.M. from triplicate repeats; \*\* $P < 0.005$ ). (c) Staining for GFP, which is co-expressed by miR-21 and miR-SCC plasmids, confirms the presence of stably transfected fibroblasts within the stroma. GFP positivity is characterised by a brown chromogenic reaction

negative regulator of MMP activity it inhibits tumour invasion.<sup>17</sup> RECK is downregulated in the majority of CRC specimens compared with normal tissue, and low expression is associated with poor outcome.<sup>35</sup> It is a membrane anchored glycoprotein and its main function is to inhibit MMP2, MMP9 and MT1-MMP activity.<sup>36</sup>

In this study, we demonstrated that miR-21 negatively regulates RECK protein expression in cultured and PCFs transfected with a miR-21/GFP co-expression plasmid.

RECK is known to regulate MMP2 via a number of post-transcriptional mechanisms and has a role in other cancer relevant biological pathways.<sup>37</sup> We demonstrated that ectopic miR-21 expression in MRC5 fibroblasts increases MMP2 activity and by using specific inhibitors to show invasion by SW480 CRC cells is MMP2 dependent, we highlighted a possible mechanism through which upregulated stromal miR-21 expression increases invasion *in vitro*. In cardiac fibroblasts, miR-21-induced MMP2 upregulation is associated with a PTEN-dependent mechanism,<sup>38</sup> and although PTEN is also a miR-21 target, we have focussed on an alternative mechanism because *in vivo* MMP2 and RECK expression are inversely correlated and have prognostic relevance in CRC.<sup>39</sup>

A description of our major findings is provided in Figure 7. In summary, we confirm that deregulation of the key oncomiR, miR-21, is a stromal phenomenon in CRC. Our data also shows that ectopic miR-21 expression in cultured fibroblasts modulates the cytotoxic impact of oxaliplatin, promotes CRC proliferation and enhances epithelial invasion. Changes in cell morphology and increased  $\alpha$ -SMA expression were observed in the immortalised MRC5<sup>21</sup> fibroblasts but not control cells (MRC5<sup>SCC</sup>). MRC5<sup>21</sup> fibroblasts also underwent myofibroblast transdifferentiation more readily in response to TGF- $\beta$  than control cells, suggesting that the functional impact of stromal miR-21 on the hallmark processes of tumour progression may be linked to the myofibroblast phenotype. Furthermore, ectopic miR-21 expression in fibroblasts resulted in downregulated RECK expression and increased MMP2 activity.

This study highlights the importance of the stroma in CRC progression and presents an interesting perspective for the development of novel, stroma-targeted drugs.

#### Materials and Methods

**Patients and samples.** Samples from patients with biopsy-proven CRC (tumour tissue and uninvolved proximal mucosa) were obtained fresh at the time

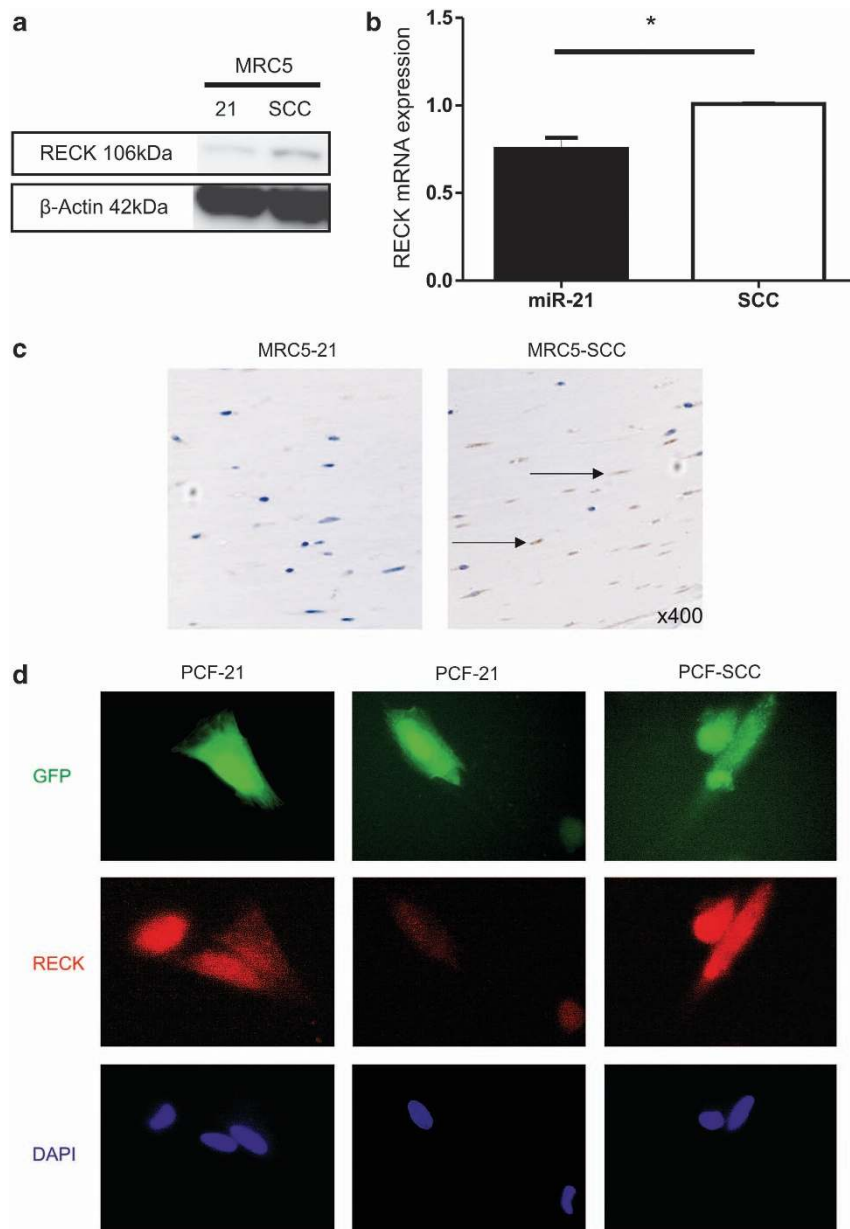


**Figure 5** MiR-21 upregulation in MRC5 fibroblasts leads to downregulated expression of MMP inhibitor RECK. (a) Western blot and (b) TaqMan qPCR analysis for RECK protein and mRNA expression in MRC5<sup>21</sup> and MRC5<sup>SCC</sup> cells; \*represents the mean  $\pm$  S.E.M. of four independent repeat experiments;  $P < 0.05$ . (c) Representative sections of organotypic stroma containing MRC5<sup>21</sup> or MRC5<sup>SCC</sup> cells immunostained with anti-RECK antibody. Positive brown cytoplasmic staining in stroma (indicated with arrows) containing MRC5<sup>SCC</sup> fibroblasts contrasts with scant RECK expression in stroma containing MRC5<sup>21</sup> cells. (d) Immunofluorescence staining for RECK in *ex vivo* PCFs transfected with either a miR-21/GFP or miR-SCC/GFP co-expression plasmid at  $\times 40$  magnification

of surgery and snap frozen in liquid nitrogen before being deposited in a designated UK Human Tissue Act-approved tumour bank. All patients provided informed consent in accordance with the Helsinki protocol and the study was approved by the regional research ethics committee. Pathological verification of diagnosis and staging was in accordance with the Association of Coloproctology of Great Britain and Ireland guidelines on the management of CRC.

Ten adenocarcinomas, with *a priori* decided tumour stage (five Dukes A and five Dukes C) and their paired uninvolved proximal mucosa were selected at random before LMD and RNA extraction.

**LMD and RNA extraction.** Frozen human tissue specimens were sectioned to 10- $\mu$ m-thickness onto membrane-mounted slides (Molecular Devices, Sunnyvale,

CA, USA). Sections were fixed in 75% ethanol, stained with 1% Cresyl Violet (Sigma, Dorset, UK) and dehydrated with increasing concentrations of ethanol before being air dried. LMD was performed using the Leica AS microdissection platform (Leica Microsystems, Milton Keynes, UK; Figure 1b) and cut stroma was collected directly into 50  $\mu$ l cell lysis buffer (RNAqueous Micro Kit, Applied Biosystems). Total RNA was extracted using the RNAqueous Micro Kit (Applied Biosystems).

**TaqMan qPCR quantitation.** Singleplex TaqMan miRNA assay reactions were performed to quantitate miR-21 expression in all 10 tumour samples. For each PCR assay, 2.5 ng of total RNA from LMD samples (0.5 ng/ $\mu$ l) was converted into cDNA using a miRNA-specific reverse transcription step according to the manufacturer's instructions (Applied Biosystems). PCR reactions were set

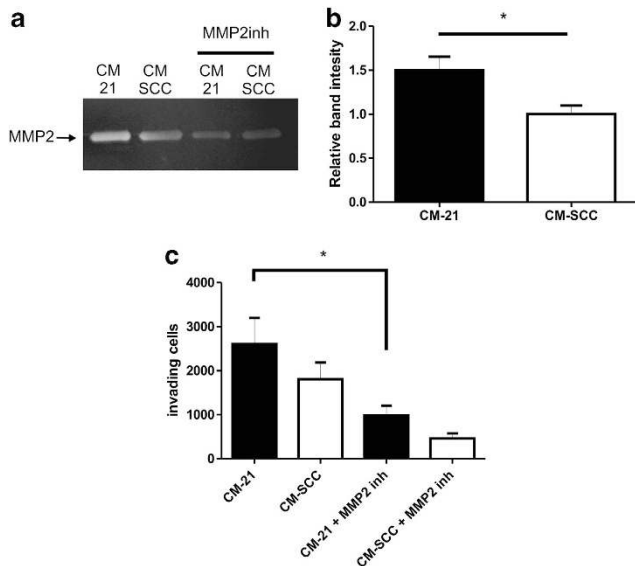


**Figure 6** Ectopic miR-21 expression in MRC5 fibroblasts leads to upregulated MMP2 activity – SW480 CRC cell invasion is MMP2 dependent. (a) Representative experiment showing zymographic activity in CM<sup>21</sup> or CM<sup>SCC</sup>, with and without MMP2 inhibitor (MMP2inh). (b) Assessment of MMP2 activity by determination of zymographical band intensity. Results are expressed as a ratio of MMP2 activity in CM<sup>SCC</sup> compared with CM<sup>21</sup> in three independent experiments. (c) Transwell invasion assay using CM<sup>21</sup> or CM<sup>SCC</sup> as chemoattractant, with and without MMP2 inhibitor. Results represent the mean number of invading cells from four repeat experiments (\**P* < 0.05)

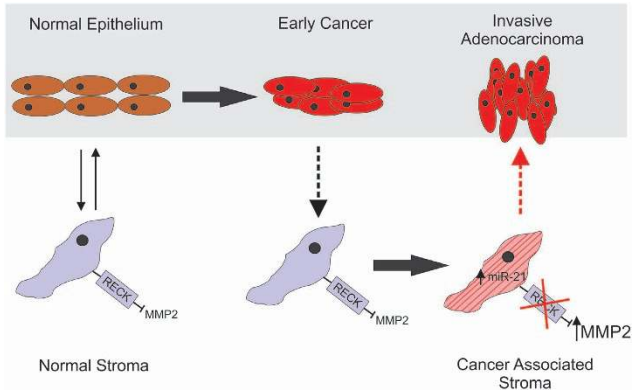


**Figure 7** Proposed impact of deregulated miR-21 expression in CRC-associated stroma. Reciprocal signalling between stromal and epithelial cells (thin black arrows; left panel) is essential for normal colonic tissue homeostasis. Early in cancer, this process is corrupted and secreted factors from transformed epithelial cells (dotted black arrow; central panel) initiate profound changes in adjacent stromal cells. Upregulated miR-21 expression in stromal fibroblasts supports TGF- $\beta$ -dependent fibroblast-to-myofibroblast transdifferentiation (thick black arrow) and causes downregulated RECK expression. Myofibroblast-derived factors are important mediators of tumour progression (dotted red arrow; right panel), and although in the absence of TGF- $\beta$ , miR-21 is not sufficient to initiate myofibroblast transdifferentiation, upregulated miR-21 does promote tumour proliferation and chemoresistance and enhanced tumour invasion through upregulated MMP2 activity

up in triplicate using miR-21-specific primers and probes and 2  $\times$  Universal PCR Master Mix (Applied Biosystems), and performed using the ABI 7500 qPCR instrument and the following cycling parameters: 95  $^{\circ}$ C for 10 min, 40 cycles of 95  $^{\circ}$ C for 15 s and 60  $^{\circ}$ C for 60 s. Expression levels were normalised to U6 snRNA,

calculated from the triplicate of  $C_T$  values using the  $\Delta\Delta C_T$  method and expressed relative to one of the specimens that was assigned the value 1.

U6B was selected as the endogenous reference gene for the purpose of miRNA validation. Mean triplicate U6B snRNA expression was quantified by the 2 –  $\Delta\Delta C_T$ , allowing expression of miR-21 to be calculated relative to this reference. Mean relative quantities were calculated for each paired tumour and normal tissue sample and a paired Student's *t*-test was performed to compare groups.

To quantify expression of epithelial and mesenchymal markers in LMD tissue, 25 ng of total RNA from the stroma or epithelium of a tumour specimen was converted to cDNA.

Subsequently, PCR reactions were set up in triplicate using specific TaqMan primers and probes for CDH1 (HS01023894\_ML) VIM (HS00185584\_ML), S100A4 (S100A4; HS00243202\_ML) and 2  $\times$  Universal PCR Master Mix, and performed using the ABI 7500 qPCR instrument and the following cycling parameters: 95  $^{\circ}$ C for 10 min, 40 cycles of 95  $^{\circ}$ C for 15 s and 60  $^{\circ}$ C for 60 s.

**In situ hybridisation.** ISH was performed as previously described.<sup>18</sup> formalin-fixed paraffin-embedded (FFPE) CRC tissue sections (6  $\mu$ m) were mounted on slides and placed in a Tecan Freedom Evo automated hybridisation instrument (Tecan, Männedorf, Switzerland) in which the following steps were performed: proteinase-K treatment using 15  $\mu$ g/ml for 8 min at 37  $^{\circ}$ C, pre-hybridisation for 15 min at 57  $^{\circ}$ C, hybridisation for 60 min at 57  $^{\circ}$ C with double DIG-labelled miRCURY LNA probes (Exiqon, Vedbaek, Denmark) for miR-21 and a scramble sequence (both at 40 nM), stringent washes with SSC buffers, DIG blocking reagent (Roche, Mannheim, Germany), alkaline phosphatase-conjugated anti-DIG (Roche), enzymatic development using NBT-BCIP substrate (Roche) for 60 min and finally nuclear fast red counterstain (Vector Laboratories, Burlingame, CA, USA).

**Cell culture and transfections.** Human CRC cell lines, SW480 and DLD1, and MRC5 lung fibroblast cell were purchased from the European Collection of Cell Culture (Salisbury, UK). Primary colonic fibroblasts were isolated and cultured as described previously.<sup>25</sup> Cells were maintained at 37  $^{\circ}$ C in a humidified atmosphere of 5% CO<sub>2</sub> in Dulbecco's modified Eagle medium (DMEM) supplemented with 10% foetal bovine serum (FBS) and 2 mM L-Glutamine.

Stable miR-21 and scrambled control (miR-SCC) miRNA expression in MRC5 fibroblasts (referred to as MRC5<sup>21</sup> and MRC5<sup>SCC</sup> cells, respectively) was achieved by transfecting precursor miRNA expression plasmids containing an IRES-driven GFP reporter and selected with puromycin (Genecopoeia, Rockville, MD, USA). PCFs were transiently transfected with miR-21 or miR-SCC plasmid by the same method. All transfections were performed using Xfect transfection reagent (Clontech Laboratories, Mountain View, CA, USA).

Triplicate organotypic models were prepared as previously described.<sup>40</sup> Briefly, 5  $\times$  10<sup>5</sup> MRC5<sup>21</sup> or MRC5<sup>SCC</sup> cells were co-cultured with SW480 CRC cells for 14 days before harvest and fixation in formalin. Paraffin-embedded sections were immunostained with anti-cytokeratin antibody to highlight CRC cells or anti-GFP antibody to highlight stably transfected fibroblasts. The middle section of each gel was imaged at  $\times$  100 magnification for the purpose of quantitation of invasion. Quantitation was achieved using Image-J image analysis software (NIH), measuring the number and area of invading tumour islands to produce a modified 'Invasion Index'.<sup>41</sup>

**Cell lysis, SDS-PAGE and western blotting.** Cells were lysed in 1  $\times$  radioimmunoprecipitation buffer (150 mM NaCl, 1% NP-40, 0.5% sodium deoxycholate, 0.1% SDS, 50 mM Tris Cl pH 7.5) in the presence of protease inhibitors (Roche). Proteins were separated under reducing conditions in 10% SDS-PAGE gels, transferred onto nitrocellulose membrane, detected with anti-RECK (Abgent, San Diego, CA, USA; AP9259c) or anti-SMA (Sigma; clone 1A4), primary antibodies and horseradish peroxidase-conjugated (Dako, Glostrup, Denmark) secondary antibody. Specific signal was visualised using Supersignal West Pico Chemiluminescent detection kit (Thermo Scientific, Rockford, IL, USA), and band intensity was quantified by densitometry using Image-J. Blots were probed for Hsc-70 or  $\beta$ -actin (Santa Cruz Biotechnology, Dallas, TX, USA) as loading controls.

**Cell proliferation and viability assay.** CM<sup>21</sup>/CM<sup>SCC</sup> were used to treat DLD1 or SW480 CRC cells plated in triplicate at a density of 5000 per well of a 96-well plate. Cell proliferation was measured using the CellTiter 96<sub>Aqueous</sub> One solution Cell Proliferation Assay (Promega, Madison, WI, USA), according to the manufacturer's instructions. Cell viability was assessed using 5  $\mu$ l of MTS



solution per well, 24 and 48 h after seeding cells. Absorbance readings at 490 nm were taken in triplicate using a spectrophotometric plate reader (Thermo Scientific, Waltham, MA, USA).

**Transwell invasion assay.** Cell invasion assays were performed over 72 h, as previously described,<sup>25</sup> using CM<sup>21</sup> and CM<sup>SCC</sup> supplemented with FBS as chemoattractant. Cells invading the lower chamber were trypsinised and counted using a Casy Cell Counter (Roche Innovatis, Bielefeld, Germany). Specific MMP2 inhibitor I (Merck, Hoddesdon, UK), prepared at a stock concentration of 10 mM in DMSO was also added to the chemoattractant at a final concentration of 25  $\mu$ M, which achieved maximal inhibition of invasion with no cytotoxic effects (data not shown).

**Apoptosis assay.** SW480 CRC cells ( $1 \times 10^5$ ) were plated overnight, in complete DMEM in triplicate wells of a 24-well plate. After 24 h, SW480 cells were washed three times with PBS and treated with 1 ml of CM<sup>21</sup> or CM<sup>SCC</sup>. A further 24 h later, cells were washed and treated either with complete DMEM containing 30  $\mu$ g/ml Oxaliplatin (Sigma, UK) or unmodified complete DMEM.

Apoptosis was examined using the Annexin V (Ann)/PI double staining method (BD Bioscience, San Jose, CA, USA). Twenty four hours after treatment (oxaliplatin or mock), SW480 cells were trypsinised without washing, resuspended in 300  $\mu$ l  $1 \times$  binding buffer (10 mM HEPES, pH 7.4, 140 mM NaCl, 2.5 mM CaCl<sub>2</sub>), pooled and double stained with 2.5  $\mu$ l Annexin V-FITC (BD Bioscience) and 2.5  $\mu$ l PI (50  $\mu$ g/ml). Ten thousand events were acquired per sample using a FACS Canto Flow Cytometer (BD Bioscience). The assay was repeated three times. Results are presented as the percentage of total cells that are viable (Ann<sup>-</sup>/PI<sup>-</sup>), early apoptotic (Ann<sup>+</sup>/PI<sup>-</sup>) or late apoptotic (Ann<sup>+</sup>/PI<sup>+</sup>).

**Gelatin zymography.** CM<sup>21</sup> and CM<sup>SCC</sup> were prepared in non-reducing  $2 \times$  SDS sample buffer and loaded without boiling to a 10% polyacrylamide gel copolymerised with 1 mg/ml of gelatin. Gels were washed twice for 30 min in 2.5% Triton X-100 (Sigma) to remove SDS and incubated in developing buffer (50 mM Tris-HCl, 0.2 M NaCl, 5 mM CaCl<sub>2</sub> and 0.02% Triton X-100) at 37 °C overnight. Gels were then stained for 30 min (0.5% Coomassie blue, 30% MeOH, 10% glacial acetic acid) before de-staining (30% MeOH, 10% glacial acetic acid). Gelatin-degrading enzymes were identified as clear bands against the dark background of the gel.

To validate the activity of miR-21 on MMP inhibition, MMP2 inhibitor I (Merck) was either added at a final concentration of 25  $\mu$ M to CM<sup>21</sup>/CM<sup>SCC</sup> for 1 h before fractionation or to developing buffer following fractionation. Images of gels were captured using a UVP Imagerstore 5000 (Ultra-Violet Products, Cambridge, UK) and band intensity quantified by Image-J. Results were expressed as relative changes in MMP activity against the scrambled control-transfected cells.

**Immunohistochemistry.** A monoclonal anti-pan-Cytokeratin antibody (Sigma) and Alexa Fluor 488 conjugate anti-GFP antibody (Invitrogen, Carlsbad, CA, USA) were used for immunohistochemistry on FFPE organotypic sections. Briefly, sections were mounted on APES-coated slides and dried for 24 h at 37 °C, and then dewaxed and rehydrated. Endogenous peroxidase was blocked for 10 min with 0.5% hydrogen peroxidase in methanol. Antigen retrieval was conducted by incubating the sections with protease (Sigma) for 10 min. Anti-pan-Cytokeratin antibody was applied in TBS (pH 7.6) overnight at 4 °C. Swine anti-rabbit IgG-biotinylated secondary antibody (Dako) was applied for 30 min, followed by peroxidase-labelled avidin-biotin complex (Vectastain Elite ABC Reagent, Vector Laboratories) for 30 min. Slides were washed three times with TBS between applications. Positive staining was visualised using DAB+ (Dako) for 5 min counterstained in Mayer's haematoxylin.

**Immunofluorescence.** Transiently transfected PCF (PCF<sup>21</sup> and PCF<sup>SCC</sup>) cells ( $5 \times 10^4$ ) were seeded in 12 wells onto 19 mm circular coverslips sterilised in 100% ethanol. After 12 h, cells were fixed in 4% paraformaldehyde for 15 min, washed three times in PBS-Triton (0.1% Triton X-100) and incubated for 30 min in 3% BSA diluted in PBS-Triton. Primary anti-RECK antibody (1/100 dilution) incubation was performed at 4 °C overnight in a humidified box. The coverslips, then, were washed three times in PBS-Triton and incubated with Alexa Fluor 546-conjugated secondary antibody (1/500) for 1 h at room temperature. Finally, coverslips were mounted onto glass slides using Vectashield Hardset mounting media with DAPI and imaged using an Olympus IX81 fluorescence microscope (Olympus, Southend-on-Sea, UK). Similar methodology was used to assess  $\alpha$ -SMA expression in MRC5<sup>21</sup> and MRC5<sup>SCC</sup> fibroblasts. Briefly, fibroblasts were

treated with complete DMEM or medium extracted from SW480 CRC cells cultured overnight in DMEM (CM<sup>SW480</sup>), or TGF- $\beta$ 1 (R&D Systems, Minneapolis, MN, USA) at final concentrations of 2 ng/ml or 10 ng/ml. Seventy-two hours later, cells were stained using anti-SMA primary antibody, counterstained and imaged. An Image-J program-based system was used for the identification and quantification of stress fibres. Briefly, the stress fibres were identified by drawing diagonal lines ( $n = 3$ ) along the images and counting sudden and sharp increases in red fluorescence intensity marking individual fibres along the lines.

**Statistical analysis.** Parametric and non-parametric statistics were expressed as mean  $\pm$  S.E.M. from multiple experiments. Statistical analysis of paired observations was conducted using Student's *t*-test or Mann-Whitney *U*-test. The threshold level of significance was set to 0.05 for all statistical tests.

### Conflict of Interest

The authors declare no conflict of interest.

1. Ferlay J, Parkin DM, Steliarova-Foucher E. Estimates of cancer incidence and mortality in Europe in 2008. *Eur J Cancer* 2010; **46**: 765–781.
2. Manfredi S, Bouvier AM, Lepage C, Hatem C, Dancourt V, Faivre J. Incidence and patterns of recurrence after resection for cure of colonic cancer in a well defined population. *Br J Surg* 2006; **93**: 1115–1122.
3. Coghlin C, Murray GI. Current and emerging concepts in tumour metastasis. *J Pathol* 2010; **222**: 1–15.
4. Hurwitz H, Fehrenbacher L, Novotny W, Cartwright T, Hainsworth J, Heim W *et al*. Bevacizumab plus irinotecan, fluorouracil, and leucovorin for metastatic colorectal cancer. *N Engl J Med* 2004; **350**: 2335–2342.
5. Cunningham D, Humblet Y, Siena S, Khayat D, Bleiberg H, Santoro A *et al*. Cetuximab monotherapy and cetuximab plus irinotecan in irinotecan-refractory metastatic colorectal cancer. *N Engl J Med* 2004; **351**: 337–345.
6. Casey TM, Eneman J, Crocker A, White J, Tessitore J, Stanley M *et al*. Cancer associated fibroblasts stimulated by transforming growth factor beta1 (TGF-beta 1) increase invasion rate of tumor cells: a population study. *Breast Cancer Res Treat* 2008; **110**: 39–49.
7. Guo X, Oshima H, Kitamura T, Taketo MM, Oshima M. Stromal fibroblasts activated by tumor cells promote angiogenesis in mouse gastric cancer. *J Biol Chem* 2008; **283**: 19864–19871.
8. De Wever O, Demetter P, Mareel M, Bracke M. Stromal myofibroblasts are drivers of invasive cancer growth. *Int J Cancer* 2008; **123**: 2229–2238.
9. De Wever O, Nguyen QD, Van Hoorde L, Bracke M, Bruyneel E, Gespach C *et al*. Tenascin-C and SF/HGF produced by myofibroblasts in vitro provide convergent pro-invasive signals to human colon cancer cells through RhoA and Rac. *FASEB J* 2004; **18**: 1016–1018.
10. Blansif JA, Caragacianu D, Alexander HR 3rd, Tangrea MA, Morita SY, Lorang D *et al*. Combining agents that target the tumor microenvironment improves the efficacy of anticancer therapy. *Clin Cancer Res* 2008; **14**: 270–280.
11. Boehm T, Folkman J, Browder T, O'Reilly MS. Antiangiogenic therapy of experimental cancer does not induce acquired drug resistance. *Nature* 1997; **390**: 404–407.
12. Winter J, Jung S, Keller S, Gregory RI, Diederichs S. Many roads to maturity: microRNA biogenesis pathways and their regulation. *Nat Cell Biol* 2009; **11**: 228–234.
13. Lu J, Getz G, Miska EA, Alvarez-Saavedra E, Lamb J, Peck D *et al*. MicroRNA expression profiles classify human cancers. *Nature* 2005; **435**: 834–838.
14. Slaby O, Svoboda M, Michalek J, Vyzula R. MicroRNAs in colorectal cancer: translation of molecular biology into clinical application. *Mol Cancer* 2009; **8**: 102.
15. Meng F, Henson R, Wehbe-Janek H, Ghoshal K, Jacob ST, Patel T. MicroRNA-21 regulates expression of the PTEN tumor suppressor gene in human hepatocellular cancer. *Gastroenterology* 2007; **133**: 647–658.
16. Asangani IA, Rasheed SA, Nikolova DA, Leupold JH, Colburn NH, Post S *et al*. MicroRNA-21 (miR-21) post-transcriptionally downregulates tumor suppressor Pdc4 and stimulates invasion, intravasation and metastasis in colorectal cancer. *Oncogene* 2008; **27**: 2128–2136.
17. Gabrieli G, Wurdinger T, Kesari S, Esau CC, Burchard J, Linsley PS *et al*. MicroRNA 21 promotes glioma invasion by targeting matrix metalloproteinase regulators. *Mol Cell Biol* 2008; **28**: 5369–5380.
18. Nielsen BS, Jorgensen S, Fog JU, Sokilde R, Christensen IJ, Hansen U *et al*. High levels of microRNA-21 in the stroma of colorectal cancers predict short disease-free survival in stage II colon cancer patients. *Clin Exp Metastasis* 2011; **28**: 27–38.
19. Yao Q, Cao S, Li C, Mengesha A, Kong B, Wei M. MicroRNA-21 regulates TGF-beta-induced myofibroblast differentiation by targeting PDCC4 in tumor-stroma interaction. *Int J Cancer* 2011; **128**: 1783–1792.
20. Gaur AB, Holbeck SL, Colburn NH, Israel MA. Downregulation of Pdc4 by miR-21 facilitates glioblastoma proliferation *in vivo*. *Neuro-oncol* 2011; **13**: 580–590.
21. Moriyama T, Ohuchida K, Mizumoto K, Yu J, Sato N, Nabae T *et al*. MicroRNA-21 modulates biological functions of pancreatic cancer cells including their proliferation, invasion, and chemoresistance. *Mol Cancer Ther* 2009; **8**: 1067–1074.

22. Liu M, Tang Q, Qiu M, Lang N, Li M, Zheng Y *et al*. miR-21 targets the tumor suppressor RhoB and regulates proliferation, invasion and apoptosis in colorectal cancer cells. *FEBS Lett* 2011; **585**: 2998–3005.
23. Seike M, Goto A, Okano T, Bowman ED, Schetter AJ, Horikawa I *et al*. MiR-21 is an EGFR-regulated anti-apoptotic factor in lung cancer in never-smokers. *Proc Natl Acad Sci USA* 2009; **106**: 12085–12090.
24. Mei M, Ren Y, Zhou X, Yuan XB, Han L, Wang GX *et al*. Downregulation of miR-21 enhances chemotherapeutic effect of taxol in breast carcinoma cells. *Technol Cancer Res Treat* 2010; **9**: 77–86.
25. Marsh D, Suchak K, Moutasim KA, Vallath S, Hopper C, Jerjes W *et al*. Stromal features are predictive of disease mortality in oral cancer patients. *J Pathol* 2011; **223**: 470–481.
26. Reis ST, Pontes-Junior J, Antunes AA, Dall'Oglio MF, Dip N, Passerotti CC *et al*. miR-21 may act as an oncomir by targeting RECK, a matrix metalloproteinase regulator, in prostate cancer. *BMC Urol* 2012; **12**: 14.
27. Valeri N, Gasparini P, Fabbri M, Braconi C, Veronese A, Lovat F *et al*. Modulation of mismatch repair and genomic stability by miR-155. *Proc Natl Acad Sci USA* 2010; **107**: 6982–6987.
28. Brabletz S, Brabletz T. The ZEB/miR-200 feedback loop—a motor of cellular plasticity in development and cancer? *EMBO Rep* 2010; **11**: 670–677.
29. Mani SA, Guo W, Liao MJ, Eaton EN, Ayyanan A, Zhou AY *et al*. The epithelial-mesenchymal transition generates cells with properties of stem cells. *Cell* 2008; **133**: 704–715.
30. Ma L, Teruya-Feldstein J, Weinberg RA. Tumour invasion and metastasis initiated by microRNA-10b in breast cancer. *Nature* 2007; **449**: 682–688.
31. Bullock MD, Sayan AE, Packham GK, Mirnezami AH. MicroRNAs: critical regulators of epithelial to mesenchymal (EMT) and mesenchymal to epithelial transition (MET) in cancer progression. *Biol Cell* 2012; **104**: 3–12.
32. Bronisz A, Godlewski J, Wallace JA, Merchant AS, Nowicki MO, Mathsyaraja H *et al*. Reprogramming of the tumour microenvironment by stromal PTEN-regulated miR-320. *Nat Cell Biol* 2012; **14**: 159–167.
33. Shibuya H, Iinuma H, Shimada R, Horiuchi A, Watanabe T. Clinicopathological and prognostic value of microRNA-21 and microRNA-155 in colorectal cancer. *Oncology* 2010; **79**: 313–320.
34. Schetter AJ, Leung SY, Sohn JJ, Zanetti KA, Bowman ED, Yanaihara N *et al*. MicroRNA expression profiles associated with prognosis and therapeutic outcome in colon adenocarcinoma. *JAMA* 2008; **299**: 425–436.
35. Takeuchi T, Hisanaga M, Nagao M, Ikeda N, Fujii H, Koyama F *et al*. The membrane-anchored matrix metalloproteinase (MMP) regulator RECK in combination with MMP-9 serves as an informative prognostic indicator for colorectal cancer. *Clin Cancer Res* 2004; **10**: 5572–5579.
36. Oh J, Takahashi R, Kondo S, Mizoguchi A, Adachi E, Sasahara RM *et al*. The membrane-anchored MMP inhibitor RECK is a key regulator of extracellular matrix integrity and angiogenesis. *Cell* 2001; **107**: 789–800.
37. Clark JC, Thomas DM, Choong PF, Dass CR. RECK—a newly discovered inhibitor of metastasis with prognostic significance in multiple forms of cancer. *Cancer Metastasis Rev* 2007; **26**: 675–683.
38. Roy S, Khanna S, Hussain SR, Biswas S, Azad A, Rink C *et al*. MicroRNA expression in response to murine myocardial infarction: miR-21 regulates fibroblast metalloproteinase-2 via phosphatase and tensin homologue. *Cardiovasc Res* 2009; **82**: 21–29.
39. van der Jagt MF, Sweep FC, Waas ET, Hendriks T, Ruers TJ, Merry AH *et al*. Correlation of reversion-inducing cysteine-rich protein with kazal motifs (RECK) and extracellular matrix metalloproteinase inducer (EMMPRIN), with MMP-2, MMP-9, and survival in colorectal cancer. *Cancer Lett* 2006; **237**: 289–297.
40. Nystrom ML, Thomas GJ, Stone M, Mackenzie IC, Hart IR, Marshall JF. Development of a quantitative method to analyse tumour cell invasion in organotypic culture. *J Pathol* 2005; **205**: 468–475.
41. Jenei V, Nystrom ML, Thomas GJ. Measuring invasion in an organotypic model. *Methods Mol Biol* 2011; **769**: 223–232.



**Cell Death and Disease** is an open-access journal published by Nature Publishing Group. This work is licensed under a Creative Commons Attribution-NonCommercial-NoDerivs 3.0 Unported License. To view a copy of this license, visit <http://creativecommons.org/licenses/by-nc-nd/3.0/>